

# Chapter 18

## Overview of Fluorescence Lifetime Measurements in Flow Cytometry

Jessica P. Houston, Zhihua Yang, Jesse Sambrano, Wenyan Li, Kapil Nichani, and Giacomo Vacca

### Abstract

The focus of this chapter is time-resolved flow cytometry, which is broadly defined as the ability to measure the timing of fluorescence decay from excited fluorophores that pass through cytometers or high-throughput cell counting and cell sorting instruments. We focus on this subject for two main reasons: first, to discuss the nuances of hardware and software modifications needed for these measurements because currently, there are no widespread time-resolved cytometers nor a one-size-fits-all approach; and second, to summarize the application space for fluorescence lifetime-based cell counting/sorting owing to the recent increase in the number of investigators interested in this approach. Overall, this chapter is structured into three sections: (1) theory of fluorescence decay kinetics, (2) modern time-resolved flow cytometry systems, and (3) cell counting and sorting applications. These commentaries are followed by conclusions and discussion about new directions and opportunities for fluorescence lifetime measurements in flow cytometry.

**Key words** Time-resolved flow cytometry, Fluorescence lifetime, Frequency-domain, Time-domain, FRET

### List of Variables:

$N^*(t)$	Number of molecules in excited state at time $t$
$k$	Sum of de-excitation rates
$k_{nr}$	Sum of radiation-less de-excitation pathways
$k_{em}$	Rate of fluorescence emission
$k_r$	Sum of radiative de-excitation pathways
$\alpha_i$	Pre-exponential factor
$E(t)$	Emission intensity as a function of time ( $t$ )
$E_0$	Maximum emission intensity
$m_{em}$	Depth of modulation of emission signal

(continued)

$\phi$	Phase of any modulated signal
$M$	Total depth of modulation for any modulated signal
$\phi_{em}$	Phase of modulated emission signal
$\phi_{ex}$	Phase of modulated excitation signal
$\Delta\phi$	Phase shift between excitation and emission modulated signals
$\omega$	Angular modulation frequency
$I(t)$	Intensity of fluorescence
$\tau$	Fluorescence lifetime of the fluorophore
$m_{ex}$	Depth of modulation of excitation signal
$a$	Laser beam height and to the velocity of a cell crossing the laser beam at $t_0$

---

## 1 Introduction

The measurement of the fluorescence lifetime with a flow cytometer is an old concept that is experiencing a re-emergence owing to new applications and advancing technologies. In fact, the earliest published and patented versions of time-resolved flow cytometry are circa 1992 [1–4]. Such demonstrations involved laboratory-constructed instruments with large, high-powered lasers and external frequency-domain laser modulation devices (discussed in later sections). Since these early demonstrations, new lasers, data systems, detector, and technologies have emerged, thus advancing how cell counters make time-resolved measurements. Included in this chapter is a discussion of these aspects of time-resolved cytometry as well as an overview of cell and microsphere experiments that utilize the fluorescence lifetime as an analysis or sorting parameter.

The fluorescence lifetime, often mathematically represented by the Greek symbol tau ( $\tau$ ), is the average time an excited fluorophore spends in an energetic state and vibrational level prior to relaxation back to a non-excited ground state. The step-wise photo-physics behind fluorescence excited state phenomena (also reviewed more descriptively later) culminate in photon emission following an exponential decay kinetic process. The timing of fluorescence decay is similar across many organic fluorophores used in life sciences and flow cytometry. Average fluorescence lifetimes range from 1 to 30 ns, and individual fluorophores might experience a shift in their average lifetime by an addition or reduction by hundreds of picoseconds (e.g., 100–1000 ps) [5]. Table 1 includes a list of the many fluorescence lifetime values measured with time-resolved flow cytometry.

**Table 1****List of fluorescence lifetimes of fluorophores that have been measured by time-resolved flow cytometry**

<b>Fluorophore/fluorescence species</b>	<b>Fluorescence lifetime (nanoseconds), citation</b>	<b>Time-resolved cytometry details</b>
Ethidium bromide (unbound)	24.0 [3]	FD, Ar-Ion 488-nm laser at 30 MHz
DNA-Check 5949 <sup>TM</sup> microspheres	6.9 [6]	FD, Ar-Ion 488-nm laser at 30 MHz
Fluorobrite 18142 microspheres	3.4 [6]	FD, Ar-Ion 488-nm laser at 30 MHz
Fluorobrite 10095 microspheres	3.5 [6]	FD, Ar-Ion 488-nm laser at 30 MHz
Immunocheck fluorospheres	7.1 [6]	FD, Ar-Ion 488-nm laser at 30 MHz
Propidium iodide (unbound)	1.3 [7]	FD, Ar-Ion 407-nm laser at 10 MHz
Propidium iodide (bound)	12.0 [7]	FD, Ar-Ion 407-nm laser at 10 MHz
Fluorescein isothiocyanate (FITC)	4.0 [7]	FD, Ar-Ion 488-nm laser at 29 MHz
Phycoerythrin-Texas Red-alpha-Thy-1.2	2.4 [8]	FD, Ar-Ion 488-nm laser at 10 MHz
Phycoerythrin (PE)	1.2 [8]	FD, Ar-Ion 488-nm laser at 10 MHz
Phycoerythrin-Cy5	1.7 [8]	FD, Ar-Ion 488-nm laser at 10 MHz
Ethidium monoazide	7.0 [8]	FD, Ar-Ion 488-nm laser at 10 MHz
7-Aminoactinomycin-D	0.7 [8]	FD, Ar-Ion 488-nm laser at 10 MHz
Phycoerythrin-alpha-Thy-1.2	1.6 [8]	FD, Ar-Ion 488-nm laser at 10 MHz
Yellow-Green <sup>TM</sup>	2.1 [9]	FD, Ar-Ion 488-nm laser at 10 MHz
Syto 9 <sup>TM</sup> green fluorescent stain	4.1 [9]	FD, Ar-Ion 488-nm laser at 10 MHz
Spherotech 8-peak Rainbow <sup>TM</sup> fluorospheres	3.9 [9]	FD, Ar-Ion 488-nm laser at 10 MHz
Teal fluorescent protein (TFP)	2.9 [10]	FD, 445-nm diode laser at 25 MHz
Dark Citrine (dCit)-TFP	1.9 [10]	FD, 445-nm diode laser at 25 MHz
Ethidium bromide (bound)	19.3 [11]	FD, 488-nm diode laser at 3 MHz
Enhanced green fluorescent protein	4.2 [12]	FD, 488-nm diode laser at 6 MHz

(continued)

**Table 1**  
**(continued)**

Fluorophore/fluorescence species	Fluorescence lifetime (nanoseconds), citation	Time-resolved cytometry details
Flow-Check <sup>TM</sup> fluorospheres	7.0 [13]	FD, 488-nm diode laser, square wave with 50% duty cycle at 5 MHz
Fluorescein	4.2 [13]	FD, 488-nm diode laser, square wave with 50% duty cycle at 5 MHz
Alexa Fluor <sup>TM</sup> 488	4.2 [13]	FD, 488-nm diode laser, square wave with 50% duty cycle at 5 MHz
Acridine orange	4.0 [13]	FD, 488-nm diode laser, square wave with 50% duty cycle at 5 MHz
Green fluorescence protein	2.7 [14]	TD, pulsed 520-nm solid state laser
di-4-ANEPPDHQ	0.2, 1.5 [14]	TD, pulsed 520-nm solid state laser

The method of acquisition is described for each lifetime measured where FD and TD describe frequency-domain and time-domain, respectively. The laser modulation for FD systems is provided and assumed sinusoidal unless otherwise noted. The values are average fluorescence lifetimes measured from a large population of cells or microspheres

A variety of biochemical factors influence fluorescence relaxation times for fluorescent molecules that are on the surface or interior of a cell. Reports show fluorescence lifetimes shorten/lengthen owing to changes in the microenvironment that surround the fluorophore such as the pH, ion concentration, temperature, or oxygen concentration [2, 15]. Additionally, the near-proximity of a fluorophore to a molecular quencher or the occurrence of energy transfer between two fluorophores will cause a shift in the average fluorescence lifetime [14, 16, 17] of one or more fluorophores involved in this process. The shortening or lengthening of the fluorescence lifetimes under different circumstances gives rise to many applications that include but are not limited to drug screening, drug delivery, contrast agent development, differentiation between spectrally overlapping fluorophores, solvent-induced relaxation experiments, collisional quenching between fluorophores, and Förster resonance energy transfer assays [8, 14, 18–20]. With fluorescence lifetime quantification, it is also possible to study basic cellular functions and phenomena such as cellular metabolism, DNA and RNA content, ATP synthesis, mitochondrial function, protein conformational changes, protein–protein interactions, protein mis-localization intracellularly, and cell signaling [10, 12, 18, 20–26]. In this chapter, we will mostly review lifetime shifts of common fluorophores used in flow cytometry, and also provide a review of fluorescence lifetimes for fluorophores that bind to micron-sized silica or polymeric spheres (i.e.,

microspheres), which are mostly used for calibration of fluorescence lifetime hardware.

The advantage of the fluorescence lifetime as a cytometry parameter is that it can be quantitative. The average fluorescence lifetime is independent of a fluorophore's excitation and emission spectrum and thus independent of the number of photons emitted by an excitable molecule as well as the total number of excitable molecules present (i.e., fluorophore concentration). Therefore, being independent of emission intensity, the fluorescence lifetime can be used to distinguish between two or more fluorophores that have similar emission spectra. In other words, the emission contribution of each fluorophore can be accounted for by the measured fluorescence lifetime and not by the sum of the detected light emitted within a wavelength bandwidth (i.e., color range). The fluorescence lifetime is also proportional to a fluorophore's quantum yield and thus a quantitative trait that can help understand the yield as a definitive contributing factor in the fluorescence "brightness" as opposed to the amount of fluorophore present, quantum efficiency, or other instrumentation variables that affect brightness.

In flow cytometry, the fluorescently labeled cell or microsphere moves through an optical excitation source at a constant velocity, limiting the amount of time fluorescence can be measured. The transit time is between 1 and 10  $\mu\text{m}$ ; therefore, nanosecond-scale fluorescence lifetimes are only measured hundreds to thousands of times before the cell departs the detector pathway. The rapid laser transit also prevents cells from being repeatedly scanned rendering the detection of lifetime gradients across the cell challenging. Therefore, reports of time-resolved flow cytometry, to-date, include measurements of average fluorescence lifetimes even though a single fluorophore may be exhibiting a range of fluorescence lifetimes within the cell or multiple fluorophores may be present and emitting in a similar spectral range.

The detection of multiple fluorescence lifetimes with a flow cytometer is discussed as an application in later sections, however it is worth noting here that this technique is common within the imaging community. That is, Fluorescence Lifetime Imaging Microscopy (FLIM) systems, which are often time-resolved adaptations of confocal and multi-photon instruments, provide multi-pixel images of fluorescence lifetime gradients across single cells. Additionally, FLIM instruments can obtain multi-exponential decay information indicating the presence of one or more fluorescence lifetime within a cell [27–31]. In contrast to FLIM instruments, time-resolved flow cytometers detect a single fluorescence lifetime; however, cytometers provide high-throughput cell sorting and counting as opposed to FLIM [9, 11, 32, 33]. Another point to be made here is that other fluorescence dynamics measurement fields (e.g., fluorimetry, spectroscopy, optical imaging, and diffuse optical tomography) measure fluorescence lifetimes through

different machinations for in vitro and in vivo use. This chapter does not review the breadth of time-resolved systems in microscopy and spectroscopy. The reader is referred to the publication by Lakowicz 2007 [34] or other publications that review fluorescence dynamics measured with non-high-throughput systems.

---

## 2 Fluorescence Lifetime Theory

The excitation of a fluorescent molecule through the absorption of light of a given energy leads to a complex relaxation process whereby excited electrons return to the ground state via a series of de-excitation processes (i.e., radiative vs. non-radiative energy release). Generally, in flow cytometry, the timing of the decay kinetic process is ignored and only the total number of photons that are released during relaxation are tracked. Therefore, cytometric instruments that can measure the rate of fluorescence decay not only integrate the total number of photons released when electrons radiatively relax to the ground state, but also clock this process, which occurs at decaying exponential rate. Much is known about the rate of decay of organic fluorophores owing to a formalized mathematical definition of fluorescence dynamics using a probabilistic viewpoint. Fluorescence decay can be represented with an ordinary differential rate equation (Eq. 1) because fluorescence follows first-order kinetics, where  $N$  is the number of excited fluorophores at time  $t$ . In this equation,  $k$  is the rate constant representing the total of all rates of the de-excitation processes including the rate of fluorescence, internal conversion, intersystem crossing, vibrational energy relaxation, and other energy dissipation processes [5, 35].

$$\frac{dN(t)}{dt} = -kN(t) \quad (1)$$

The sum of  $n$  number of rate constants can be represented by Eq. 2, and all are equivalent to either nonradiative ( $k_{nr}$ ) or radiative processes ( $k_r$ ). In other words, the summation is the total of all kinetic rate constants representing energy dissipation.

$$k = k_1 + k_2 + k_3 + k_4 + \dots + k_n \dots = k_r + k_{nr} \quad (2)$$

Experimentally we observe that relaxation of the electrons from an excited state(s) occurs following first-order kinetics, which is approximated by the solution to Eq. 1, shown here in Eqs. 3 and 4, which represent decay based on:  $N$  number of fluorophores decayed, or the fluorescence intensity decay,  $I$ , following excitation with an initial intensity,  $\alpha$ .

$$N(t) = N(0) \cdot e^{-kt} \quad (3)$$

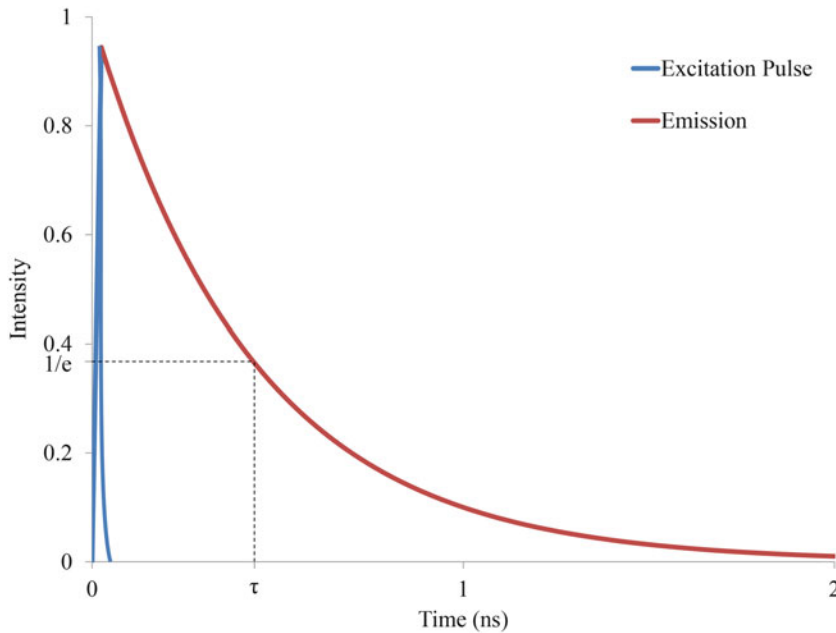


**Fig. 1** Graphical representation of time-domain approaches to fluorescence lifetime measurements: a pulsed laser (*blue*) is used to excite the cell and/or fluorescent particle. The intensity of the fluorescence emission by the excited sample (*red*) decreases in an exponential fashion as a function of time. The lifetime is defined when the intensity decreases to  $1/e$

$$I(t) = \alpha \cdot e^{-t/\tau} \quad (4)$$

Equation 4 follows what is observed experimentally in which light of a high intensity but small pulse width,  $I(0)$ , or  $\alpha$ , is used to excite a fixed amount of fluorophore molecules at an initial time,  $t = 0$ . The resulting fluorescence emission at time,  $t$ , is therefore  $I(t)$ , and decays exponentially. Figure 1 illustrates this with a graph of the initial pulse of light (i.e., simulation with a delta function) and resulting fluorescence decay.

Equation 4 is in terms of the fluorescence lifetime,  $\tau$ , which is the time for the emission intensity to reach  $1/e$  of the original excitation value, or for the number of relaxed molecules to reach 36.8% of the total number of excited fluorophores.

The fluorescence lifetime full representation is:

$$\tau = \frac{1}{k} = \frac{1}{(k_{em} + k_{nr})} \quad (5)$$

where  $k_{em}$  is the rate constant for radiative decay through fluorescence emission. During any multi-exponential decay process that might occur (e.g., emission by a mixture of fluorophores with different fluorescence lifetimes), the equation can be restated as a summation of first-order decay kinetic events. The addition accounts for each type of fluorophore, which collectively emit and

contribute to the total signal. Equation 6 provides this summation where  $\alpha_i$  is the initial excitation intensity absorbed by each specie,  $i$ , and  $\tau_i$  is the fluorescence lifetime corresponding to that specie.

$$I(t) = \sum_{i=1}^n \alpha_i \cdot e^{-t/\tau_i} \quad (6)$$

---

### 3 Time-Resolved Flow Cytometry

Two general methods are taken to make flow cytometers able to measure single or multiple fluorescence decay kinetics. Collectively, the methods are considered *time-resolved* and subsequently categorized as either time-domain or frequency-domain approaches.

Frequency-domain measurements are common because the methodology minimizes the hardware and signal processing modifications necessary for fluorescence lifetime transformation. Frequency-domain measurements involve sinusoidal (or square wave) modulation of the laser excitation source at a radio frequency (RF) of 1–100 MHz. When a fluorescently labeled cell is excited with this type of sinusoidal modulation, the intensity of emitted light, which decays as an exponential function of time (*see* Eq. 4), carries the same modulation frequency. However, the amplitude is attenuated and the phase is shifted owing to the fluorescence decay kinetics. Figure 2 illustrates this concept, where a high-frequency modulated excitation signal is plotted with a sinusoidal emission signal, which has the same modulation but a shift in phase and attenuation of the RF amplitude. The fluorescence lifetime is calculated from the information in the modulated signal using (generally) a Fourier transformation of the exponentially decayed function which depends on time. As shown by Eq. 7, the frequency-domain representation of the modulated emission intensity,  $E(t)$ , can be represented by a harmonic function which depends on angular modulation frequency ( $\omega$ ), phase ( $\phi$ ), and modulation amplitude ( $m_{cm}$ ). If the harmonic modulation follows a square wave shape, as opposed to sinusoidal, Eq. 8 is modified to represent a square wave as a summation of multiple odd harmonics (*see* Jenkins et al. for a thorough description [13]).

$$E(t) = E_0[1 + m_{cm} \sin(\omega t - \phi)] \quad (7)$$

Both the amplitude and phase of the emission signal are compared to the amplitude and phase of the excitation signal in order to find the amplitude demodulation and phase shift between these two signals (excitation and emission). This step is important because both values are proportional to the fluorescence lifetime.

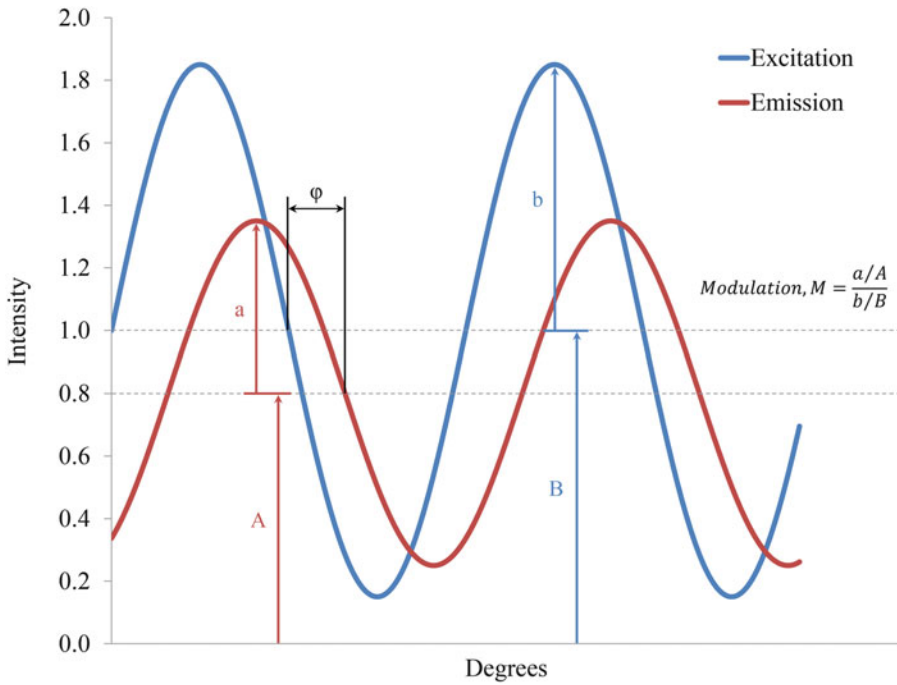


**Fig. 2** Graphical representation of the frequency-domain method for the fluorescence lifetime measurement. The measurement is conducted using a radio-frequency modulated excitation signal (*blue*). The subsequent emission is modulated at the same angular frequency but delayed in phase ( $\phi$ ) and amplitude demodulated ( $M$ ). The excited state lifetime can be determined by using phase delay and demodulation

The relationships between the fluorescence lifetime and amplitude demodulation,  $M$ , and phase shift,  $\Delta\phi$ , are provided in Eqs. 8 and 9. The demodulation is calculated by dividing the modulation depth of the emission signal by modulation of excitation. The phase shift,  $\Delta\phi$ , is found by subtracting the emission phase from the excitation phase, which is measured with the side scatter signal in flow cytometry.

$$M = \frac{1}{\sqrt{1 + (\omega\tau)^2}} \quad \text{or} \quad \tau = \frac{\sqrt{\left(\frac{m_{sc}^2}{m_{em}^2} - 1\right)}}{\omega} \tag{8}$$

$$\tau = \frac{\tan \Delta\phi}{\omega} \tag{9}$$

The frequency-domain concept in the context of a flow cytometry process is also graphically illustrated in Fig. 3. The continuous wave yet modulated excitation source is focused onto fluorescently labeled moving cells, which are counted as they cross the laser beam and emit amplitude-attenuated and phase-shifted fluorescence. As seen in Fig. 3, the signal that is detected is Gaussian in shape and superimposed with an RF component. The Gaussian shape is a result of simulating a Gaussian mode laser output with

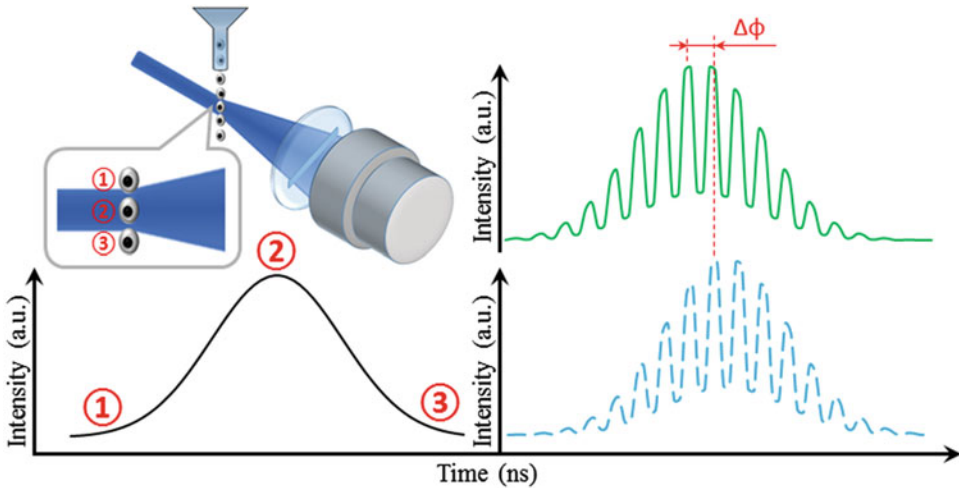


**Fig. 3** (Top left) Fluorescent particles or cells (small circular shapes) pass through a continuous laser beam and the result is an emission or light scatter signal that increases and decreases to resemble a Gaussian shape (bottom left). The illustration depicts the signal rise and fall dependent on the particle’s position in the laser beam. The particle is partially illuminated at position 1 when entering the laser beam, generated signal achieves highest intensity of the Gaussian profile when particle reaches position 2 and gradually decreases to 0 when particle leaves the laser beam at position 3. (Right panel) Representative fluorescence and side-scatter waveforms that result with frequency-domain flow cytometry. The phase shift ( $\Delta\phi$ ) between the reference (side-scatter channel) and the emission signal is used to compute the average fluorescence lifetime

a spherical particle passing through the perfectly aligned beam at an ideal laminar velocity profile. Equation 7 is a mathematical approximation of the emission collected by a flow cytometer, combining both the sinusoidal component as well as the Gaussian function:

$$E(t) = E_0[1 + m_{em} \sin(\omega t - \phi_{em})] \cdot e^{-a^2(t-t_0)^2} \quad (10)$$

The calculation of the fluorescence lifetime in flow cytometry requires digitization of fluorescence emission as well as an excitation reference signal. Therefore, the correlated side scattered light signal (mathematical approximation in Eq. 11) is used as the reference.

$$E(t) = E_0[1 + m_{ex} \sin(\omega t - \phi_{ex})] \cdot e^{-a^2(t-t_0)^2} \quad (11)$$

The digitized signals represented by Eqs. 10 and 11 are processed with a discrete Fourier Transform, Goertzel algorithm, non-linear regression, or other favored signal processing step that results in an accurate measure of the phase and amplitude of each correlated waveform for all cells measured. The type of digital signal processing will vary depending on the speed required to calculate the fluorescence lifetime as a real-time parameter for cell counting and/or cell sorting [9, 36].

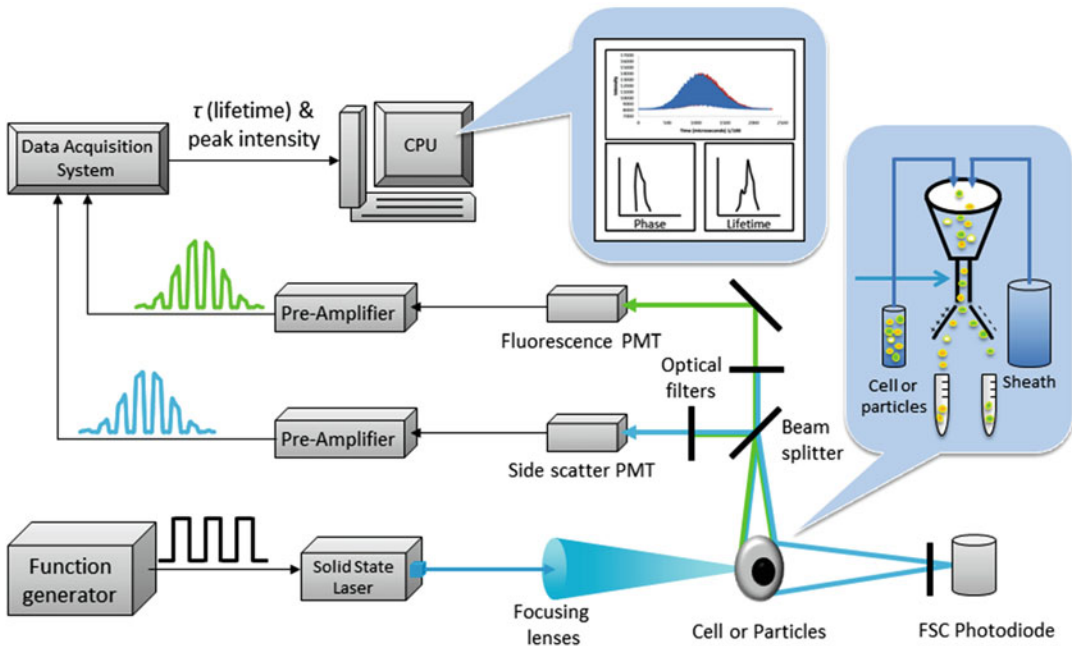


**Fig. 4** Schematic that illustrates the basic components of a frequency-domain flow cytometer. The instrument depicted might be a result of a retrofitted commercial flow cytometer or “home-built” system. Cells passing through a square-wave and digitally modulated laser diode emit fluorescence and side scatter, which are detected by photomultiplier tubes (PMTs). The PMT output is routed to high frequency preamplifiers and subsequently digitized directly with a high speed digital data acquisition system. Either real-time or off-line histograms are formed using digital signal processing or calculations off-line with MATLAB, for example

Figure 4 is an illustration schema of frequency-domain flow cytometry. In this schematic, the laser modulation is represented by a square wave function with a fundamental RF frequency. Among a variety of ways to optimize frequency-domain instruments, one important consideration is the photoelectron transit time spread of the photo-multiplier tube detectors. A PMT specified with a minimum spread is optimal for the output response when short pulses, or rapidly modulating light are collected. Additional considerations are the use of solid state laser diodes that can be directly modulated, the need for preamplifier with high frequency capabilities, as well as data acquisition systems with digitization rates compatible with MHz frequencies.

Frequency-domain systems were first introduced as “phase-sensitive flow cytometry” [1, 37–39], taking the form of analog homodyning systems. A thorough review of the operation of these instruments is provided by Houston et al. (2012) [36]. Briefly, phase-sensitive flow cytometry led to a range of instrumentation capabilities and configurations including early versions of digital lifetime acquisition at one modulation frequency (20-MHz), simultaneous modulation of laser excitation at 16-MHz and 45-MHz,

and many demonstrations with labeled cells and microspheres [6, 8, 16, 21, 40–42]. Some examples toward the advancement of frequency-domain flow cytometry include work by Jenkins et al., Sands et al., and Cao et al. [10, 11, 43]. Jenkins and colleagues leveraged square wave RF laser modulation to extract multiple phase shifts from the multiple odd harmonics that result when a square wave is decomposed with Fourier methods. Sands and Cao introduced the use of the phasor plot in flow cytometry. A phasor plot combines the phase shift,  $\phi$ , and demodulation,  $M$ , parameters from a frequency-domain fluorescence measurement. Within a phasor plot, points on a graph are at a radial distance from the pole, which is equal to the measured demodulation. The angle between the phasor axis ( $x$ -axis) and the radius is called the phasor angle, which is equal to the angle of phase shift (*see* Fig. 5). Presenting data in this fashion provide a visual tool to reveal differences in fluorescence lifetimes as a result of the phase shift and demodulation values. The FLIM and fluorimetry community have been implementing phasor plots for several years [27, 44, 45] because of the ease with which one can visualize distributions of

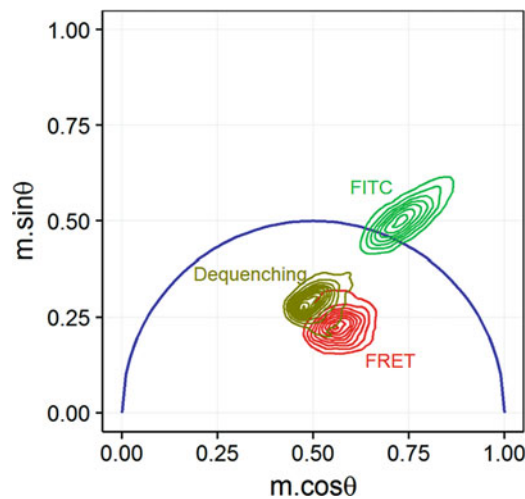


**Fig. 5** A MATLAB-generated phasor plot. The graph is an  $x$  vs  $y$  polar plot and is a common lifetime visualize tool in FLIM and is now emerging in time-resolved flow cytometry. In this figure, a simulation was performed with frequency-domain modulation of 25 MHz and two independent fluorescence lifetimes (19 and 4-ns). The points located on semicircle are vectors with magnitude and directions which equal the demodulation and phase shift, respectively. The points that fall on the semicircle represent signals from single exponential fluorescence decay kinetics. A line joining two of the simulated single fluorescence lifetime points is added to show where any other vector (phase and modulation component of a fluorescence signal) might be located if the fluorescence lifetime falls in between the single lifetime values which the line connects (i.e., between 4 and 19 ns)

multiple lifetime components taken from an image of a group of cells. The pseudophasor plot was first introduced in flow cytometry for cell sorting [10]. The pseudophasor plot graphs the real and imaginary components of the Fourier output as a 2-D histogram so that sort gates can be based on values that are dependent on fluorescence decay kinetics.

In other frequency-domain cytometry advancements, phase-filtering and microfluidic systems were developed. The phase-filtering approach is an adaptation of phase and modulation measurements; it provides a way to sort cells based on a fluorescence lifetime value under conditions where the entire cell population expresses equal fluorescence output (i.e., color and intensity). The approach is performed with population distributions whereby the entire cell suspension emits at similar emission levels, yet a fraction of the population has a different fluorescence lifetime, perhaps owing to the presence of a particular biochemical or molecular feature present within that smaller percentage of cells. Thus phase-filtering will enable the isolation and sorting of the desired cell fraction by collecting the phase-shifts cell-by-cell and processing the values with frequency-domain mixing hardware and subsequently connecting to a sorting instrument's data acquisition board [11]. In other modern frequency-domain cytometry systems, microfluidic chips were combined with RF laser modulation sources and aligned in a sequential manner in order to alternate bright and dark zones for cells to pass through. In one example, the laser excitation sources were aligned in series for fluorescent protein photobleaching studies and to understand the unique excited state kinetics (i.e., ground state depletion) of protein variants [32, 33, 46].

The second form of time-resolved flow cytometry involves time-domain methods; methods that are not frequency-domain are categorized herein as time-domain. With time-domain approaches, the fluorescence decay is observed over time with single photon counting detectors, then measured and fit using single or multiple exponential decay functions. The measurement is practiced by pulsing the excitation laser source and with precise timing collecting the emission photons after laser pulsation. The decaying emission is collected by gating a detector, which involves activating its photosensitivity simultaneous to laser pulsation and then deactivating the detector after a short time for photons to be counted during fluorescence decay. This method when integrated with flow cytometry hardware requires precise timing and is coupled with off-line analyses to fit exponential decay data and provide a fluorescence lifetime output, which can then be turned into a cytometric parameter and plotted in a histogram format.

Some recent examples of time-domain cytometry systems are described herein. In 2013, Li et al. developed a pseudo-time-resolved system with a "fluorescence lifetime excitation cytometry by kinetic dithering" (FLECKD) instrument. The system takes

hydrodynamically focused cells and rapidly moves a finely focused laser across each cell multiple times before the cell exits the detection region. This essentially “dithers” the laser via an acousto-optic deflector so rapidly that the result is similar to pulsing the laser [47]. The pulse width of the dithered laser is approximately 25-ns FWHM, and the beam is moved approximately 10–20 times across each moving cell. With the FLECKD instrument, Li et al. were able to observe single exponential fluorescence decays for a range of fluorescent microspheres and cells. Figure 6 is a figure adapted from Li et al. to illustrate this concept. Recently, Nebdal et al. modified an automated microscope platform and combined it with a microfluidic chip in order to extract fluorescence decay kinetics of cells passing through the microfluidic channels [14]. A picosecond pulsed laser source excited each sample, and time-correlated single photon counting (TCSPC) was performed with a detector. Off-line analysis using non-linear regression permitted acquisition of fluorescence lifetimes. Similarly, time-domain cytometry examples described in the literature [48–50] include CCD detectors that are gated to collect emission over longer times (i.e., milliseconds). Cytometry systems that collect the timing of phosphorescence have

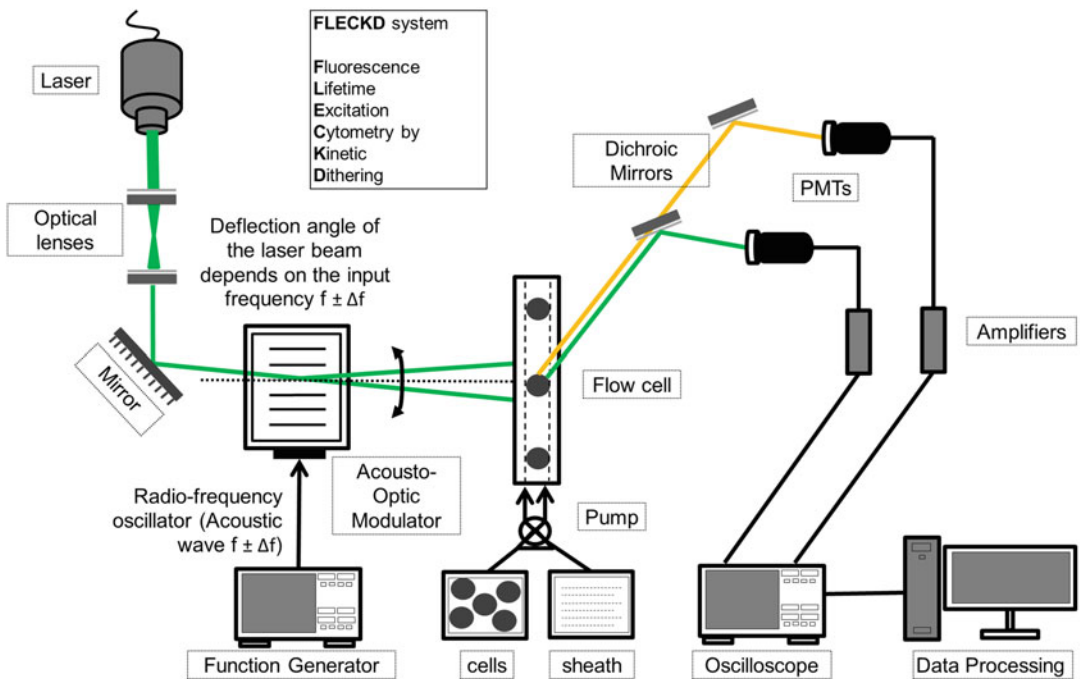


**Fig. 6** Schematic of the fluorescence lifetime excitation by kinetic dithering (FLECKD) system. A continuous laser beam is focused onto an acoustic-optic deflector, which dithers the laser beam across the flow cell in a lateral direction multiple times as the event (i.e., cell or microsphere) is moving. This system acquires data with an oscilloscope, however a high data acquisition system is a possible way to collect data in real-time for the cytometric throughput

been developed using CCD camera systems, and are mentioned here because of the high-throughput nature and time-domain approach.

A recent report by Cao and colleagues showed the ability to measure average fluorescence lifetimes [51] with an approach that is neither time-domain nor frequency-domain per se. The premise was to use cytometry to measure the fluorescence lifetime with neither pulsed nor modulated lasers. Demonstrations were validated where cytometry data in the form of standard waveforms were processed for the inherent information they carry, which leads to a calculation of the average fluorescence lifetime cell-by-cell at a nominal cytometric throughput. The fluorescence lifetime was proven to be proportional to the average peak-to-peak pulse delay between correlated fluorescence and scattered light signals. Signal processing steps were tested to see which algorithm best fit the cytometrically collected Gaussian-like waveforms. The promising aspect of this paradigm is that it shows how any existing commercial instrument is inherently capable of detecting average fluorescence lifetime measurements. As described, there are many versions of time-resolved flow cytometers and expectedly many more applications. The section that follows provides a summary of the single cell analyses performed with systems such as those described previously.

---

## 4 Applications of Time-Resolved Flow Cytometry

Single cell counting and sorting applications of time-resolved flow cytometry range from measurement of exogenous fluorophores to fluorescent proteins. Each application ranges in purpose and advantage, and provides unique methods for understanding intracellular phenomena. Table 2 provides a comprehensive list of a variety of time-resolved applications where fluorescence lifetimes were reported for a variety of cell or microsphere measurements.

### 4.1 Exogenous Fluorophores and Microspheres

Early time-resolved flow cytometry experiments (pre-2000s) concentrated on fluorescence lifetime measurements of propidium iodide (PI), ethidium bromide (EB), and fluorescein isothiocyanate (FITC), all of which are organic fluorophores that intercalate into nucleic acids or proteins after cellular fixation. PI, EB, and FITC have average fluorescence lifetimes of 12.0-, 19.3-, and 4.0-ns, respectively [3, 7, 19–21, 23, 40, 53, 54] and which depend on how they are bound to molecules within the cell. For example, phase-sensitive flow cytometry instruments measured the fluorescence lifetime shift of EB, which changes when intercalated into nucleic acids. Phase-sensitive flow cytometers also measured the fluorescence lifetime of PI when it nonspecifically binds to proteins within fixed cells. The fluorescence lifetime of FITC was measured

**Table 2**  
**Chronological listing of the various time-resolved flow cytometry instruments and applications described in the literature**

<b>Year, citation</b>	<b>Title of time-resolved cytometry instrument development and/or application</b>	<b>Approach</b>
1993 [1]	A flow cytometer for resolving signals from heterogeneous fluorescence emissions and quantifying lifetime in fluorochrome-labeled cells/particles by phase-sensitive detection	Frequency domain
1993 [4]	Resolution of fluorescence signals from cells labeled with fluorochromes having different lifetimes by phase-sensitive flow cytometry	Frequency domain
1993 [2]	Fluorescence lifetime-based sensing of pH, Ca <sup>2+</sup> , K <sup>+</sup> and glucose	Frequency domain
1993 [3]	Phase-resolved fluorescence lifetime measurements for flow cytometry	Frequency domain
1994 [39]	Phase-sensitive detection methods for resolving fluorescence emission signals and directly quantifying lifetime	Frequency domain
1994 [6]	Fluorescence lifetime measurements in a flow cytometer by amplitude demodulation using digital data acquisition techniques	Frequency domain
1995 [40]	Simultaneous dual-frequency phase-sensitive flow cytometric measurements for rapid identification of heterogeneous fluorescence decays in fluorochrome-labeled cells and particles	Frequency domain
1996 [16]	Analysis of fluorescence lifetime and quenching of FITC-conjugated antibodies on cells by phase-sensitive flow cytometry	Frequency domain
1996 [52]	Time-resolved fluorescence-decay measurement and analysis on single cells by flow cytometry	Time domain
1996 [21]	Interactions of intercalating fluorochromes with DNA analyzed by conventional and fluorescence lifetime flow cytometry utilizing deuterium oxide	Frequency domain
1997 [18]	Monitoring uptake of ellipticine and its fluorescence lifetime in relation to the cell cycle phase by flow cytometry	Frequency domain
1997 [20]	Differential effects of deuterium oxide on the fluorescence lifetimes and intensities of dyes with different modes of binding to DNA	Frequency domain
1998 [41]	Flow cytometric fluorescence lifetime analysis of DNA-binding probes	Frequency domain
1998 [53]	Fluorescence lifetime measurement of free and cell/particle-bound fluorophore by phase-sensitive flow cytometry	Frequency domain
1998 [23]	Apoptosis induced with different cycle-perturbing agents produces differential changes in the fluorescence lifetime of DNA-bound ethidium bromide	Frequency domain
1998 [41]	Flow cytometric characterization and classification of multiple dual-color fluorescent microspheres using fluorescence lifetime	Frequency domain
1999 [7]	Fluorescence intensity and lifetime measurement of free and particle-bound fluorophore in a sample stream by phase-sensitive flow cytometry	Frequency domain

(continued)

**Table 2**  
**(continued)**

<b>Year, citation</b>	<b>Title of time-resolved cytometry instrument development and/or application</b>	<b>Approach</b>
1999 [54]	Enhanced immunofluorescence measurement resolution of surface antigens on highly autofluorescent, glutaraldehyde-fixed cells analyzed by phase-sensitive flow cytometry	Frequency domain
1999 [8]	Discrimination of damaged/dead cells by propidium iodide uptake in immunofluorescently labeled populations analyzed by phase-sensitive flow cytometry	Frequency domain
1999 [24]	Simultaneous analysis of relative DNA and glutathione content in viable cells by phase-resolved flow cytometry	Frequency domain
2000 [8]	Flow cytometric, phase-resolved fluorescence measurement of propidium iodide uptake in macrophages containing phagocytized fluorescent microspheres	Frequency domain
2001 [25]	Time-resolved fluorescence measurements	Frequency domain
2003 [26]	Fluorescence lifetime-based discrimination and quantification of cellular DNA and RNA with phase-sensitive flow cytometry	Frequency domain
2006 [55]	Effect of polystyrene microsphere surface to fluorescence lifetime under two-photon excitation	Time domain
2007 [56]	Practical time-gated luminescence flow cytometry. I: concepts	Time domain and frequency domain
2010 [9]	Digital acquisition of fluorescence lifetime by frequency-domain flow cytometry	Frequency domain
2010 [57]	Resolving multiple fluorescence decays from single cytometric events	Frequency domain
2011 [43]	Flow cytometric separation of spectrally overlapping fluorophores using multifrequency fluorescence lifetime analysis	Frequency domain
2012 [36]	Capture of fluorescence decay times by flow cytometry	Frequency domain
2012 [32]	Microfluidic flow cytometer for quantifying photobleaching of fluorescent proteins in cells	Micro fluidic
2012 [58]	Time-gated orthogonal scanning automated microscopy (OSAM) for high-speed cell detection and analysis	Time domain
2012 [59]	Microfluidic sorting of microtissues	Micro fluidic
2013 [11]	Cytometric sorting based on the fluorescence lifetime of spectrally overlapping signals	Frequency domain
2013 [12]	Subcellular localization-dependent changes in EGFP fluorescence lifetime measured by time-resolved flow cytometry	Frequency domain
2014 [10]	Measuring and sorting cell populations expressing isospectral fluorescent proteins with different fluorescence lifetimes	Frequency domain
2014 [51]	Expanding the potential of standard flow cytometry by extracting fluorescence lifetimes from cytometric pulse shifts	Non time/frequency domain

(continued)

**Table 2**  
**(continued)**

<b>Year, citation</b>	<b>Title of time-resolved cytometry instrument development and/or application</b>	<b>Approach</b>
2014 [47]	Fluorescence lifetime excitation cytometry by kinetic dithering	Time domain
2014 [49]	Tunable lifetime multiplexing using luminescent nanocrystals	Time domain
2014 [60]	High-throughput measurement of the long excited-state lifetime of quantum dots in flow cytometry	Frequency domain
2014 [48]	On-the-fly decoding luminescence lifetimes in the microsecond region for lanthanide-encoded suspension arrays	Time domain
2014 [46]	Microfluidic flow cytometer for multiparameter screening of fluorophore photophysics	Frequency domain and micro fluidic
2014 [61]	High-throughput time-correlated single photon counting	Time domain and micro fluidic
2014 [62]	À la fizeau in flow: pulse shape-assisted fluorescence lifetime	Frequency domain
2015 [13]	Toward the measurement of multiple fluorescence lifetimes in flow cytometry: maximizing multi-harmonic content from cells and microspheres	Frequency domain
2015 [14]	Time-domain microfluidic fluorescence lifetime flow cytometry for high-throughput Förster resonance energy transfer screening	Time domain and micro fluidic
2015 [50]	Tuning upconversion luminescence lifetimes of KYb2F7: Ho <sup>3+</sup> nanocrystals for optical multiplexing	Time domain
2015 [63]	High-speed multiparameter photophysical analyses of fluorophore libraries	Frequency domain and micro fluidic
2015 [33]	Time and frequency-domain measurement of ground-state recovery times in red fluorescent proteins	Time domain and frequency domain
2015 [64]	A high-throughput direct fluorescence resonance energy transfer-based assay for analyzing apoptotic proteases using flow cytometry and fluorescence lifetime measurements	Frequency domain

when conjugated to antibodies and bound to cell surface receptors [16]. The phase-sensitive flow cytometry measurements of PI, EB, and FITC involved fluorescently labeled mammalian cell cultures (e.g., Chinese hamster ovary, mouse thymus) and in some cases these fluorophores were measured when imbibed into microspheres [21, 25, 40]. A notable example of phase-sensitive cell counting includes the measurement of DNA content in the presence of RNA. The fluorescence lifetime of EB when intercalated into DNA is different and distinct from RNA, and therefore provides an alternative for cell cycle measurements [25, 26].

In general, there have been a wide range of time-resolved flow cytometry studies involving bright, exogenous organic

fluorophores that are bound to fixed or viable cells. The purpose of each lifetime study varies, and they are too numerous to describe herein. Refer to Table 2 for a chronological overview of different applications. Some examples include work discovering the effects of deuterium oxide on the decay kinetics of EB, monitoring DNA and glutathione content with Hoechst 33342 and monobromobimane; discriminating damaged vs. dead cells using PI, detecting bound from un-bound cell surface receptors with FITC, and determining the order of the bi-layer lipid membrane with a lipophilic dye, di-4-ANEPPDHQ [16, 18, 23, 26, 42, 65]. The overall goal of many time-resolved measurements is to show that the fluorescence lifetimes provide a means to discriminate intracellular markers that are otherwise non-detectable with fluorescence intensity-only cytometry.

#### **4.2 Fluorescent Proteins**

In addition to the bright and commonly used organic fluorophores, a variety of fluorescent proteins (FPs) have been measured with time-resolved flow cytometry. The expression of fluorescent proteins in single cells contributes to functional cellular information that can be obtained with a flow cytometer such as protein–protein interactions, protein conformation, protein movement, gene expression, and cell signaling, for example. With time-resolved cytometry, the fluorescence lifetime of the expressed proteins adds a quantitative parameter owing to the fact that FPs generally have lower quantum yields, broad emission spectra, weaker fluorescent signals, and are susceptible to photobleaching. For example, time-resolved flow cytometry might discriminate between the dim FP signal and autofluorescence background, which can be an issue in flow cytometry (i.e., complicates compensation).

Fluorescent proteins might also experience quenching or excited state lifetime shifts when exposed to different microenvironments and therefore can indirectly indicate intracellular biochemistry. For example, a time-resolved experiment explored the ability to measure GFP position within a cell by inducing GFP movement from diffuse cytoplasmic expression to collective aggregates during autophagy. GFP was fused to LC3 protein, which localizes within autophagosomes during the autophagy process. The fluorescence lifetime was measured when GFP was diffusely expressed in the cell and when it was collected into the punctate regions. The average fluorescence lifetime shortened by 0.4 ns during autophagy [12]. The benefit of measuring protein movement in the context of autophagy is the potential for high-throughput screening of compounds that might inhibit or affect autophagy using the GFP lifetime as a metric for reporting the stage of autophagy. In other fluorescent protein studies, complex fluorescence dynamics were studied with red fluorescent proteins and measured with frequency-domain flow cytometry [32]. The RFP expressers were evaluated for irreversible and reversible

photobleaching phenomena as well as characterization of [46] photostability and photoactivatable features [33].

Fluorescent protein expression in cells measured with flow cytometers is often coupled with cell sorting. Therefore, if sort gates depend on fluorescence lifetime parameters, cell populations can be separated based on quantitative FRET efficiencies, quantum yields of the proteins, and dim protein expressers. In a recent example, fluorescent protein fusions in *Saccharomyces cerevisiae* were expressed and cells were sorted based on the measured excited state lifetimes [10]. The yeast cell study took average fluorescence lifetimes of teal fluorescent protein (TFP) and TFP when fused to dark-state Citrine fluorescent protein (dCit). Fluorescence lifetime differences existed owing to non-radiative energy transfer within the TFP-dCit construct as compared to TFP alone. Yet, the difference in the TFP vs TFP-dCit emission signal alone was not enough to sort *S. Cerevisiae* cell populations. Whereas the fluorescence lifetime-dependent parameters led to clearly distinct subpopulations when graphically represented by a pseudo-phasor plot. Described in previous sections, a phasor plot is analogous to a 2-D histogram where each event (i.e., dot) is positioned on the quadrant by the measured angle and magnitude, which are functions of fluorescence lifetime. In this example, cell sorts were possible based on fluorescence dynamics of the proteins expressed in cells when the fluorescence intensity was not enough to separate the subpopulations. However, sorting based on the fluorescence lifetime of proteins has another added benefit in that it provides a new approach for screening and isolating protein variants with high quantum yields. In a short report, Yang et al. described how the fluorescence lifetimes of near-infrared fluorescent proteins (iRFPs) expressed in *Escherichia coli* can be used to isolate variants with high quantum yields [66]. During the development of iRFP libraries, it is valuable to have a high-throughput sorting instrument that can separate cells with high quantum yield variants. The quantum yield is proportional to the fluorescence lifetime, thus a sorting parameter that can be used to isolate bright and stable proteins from those that appear bright for other reasons (i.e., quantum efficiency, number of FP molecules present, instrumentation artifacts). Overall fluorescent protein measurements with cytometry can benefit from fluorescence lifetime measurements, particularly in cases that involve energy transfer and protein interactions.

### **4.3 Förster Resonance Energy Transfer**

A number of recent time-resolved applications either with or without fluorescent proteins have involved Förster resonance energy transfer (FRET) bioassays. FRET is a non-radiative energy transfer event between a fluorescent donor and fluorescent acceptor molecule. The fluorescence lifetime is a quantitative metric for FRET

because the donor fluorescence lifetime shortens by several hundred picoseconds when it is quenched by energy transfer with the acceptor molecule [5, 14, 30, 64, 67]. FRET efficiencies are validated by measuring average fluorescence lifetime [17], and therefore make precise measurements of protein-to-protein interactions or protein conformational changes [68–70]. One of the first demonstrations of FRET measured by time-resolved flow cytometry involved a study to screen the expression of caspases that are involved in apoptosis. Suzuki and co-workers labeled cells with fluorescent proteins (e.g., GFP, RFP) and exogenous fluorophore (Alexa dyes) FRET pairs. The FRET pairs, or “*bioprobes*,” were linked by peptide sequences that were cleavable by caspase enzymes. Therefore, the bioprobes provided an indirect measure of caspase levels during apoptosis induction [64]. Other time-resolved FRET measurements in flow cytometry include GFP-RFP fusions linked by different lengths of peptide bridges. FRET efficiencies between GFP and RFP were measured using fluorescence lifetime changes, and were expectedly different depending on the length of the oligopeptide linker. In the same study, FRET efficiencies were measured by detecting GFP lifetime shortening when engaged in FRET with Cy3. An epidermal growth factor receptor (EGFR)-bound GFP interacted with an anti-phosphotyrosine antibody-bound Cy3 fluorophore. The study evaluated the activation of epidermal growth factor receptor tyrosine phosphorylation because the Cy3 bound antibody was recruited to the phosphorylated tyrosine site on EGFR and therefore was able to engage in FRET with the GFP [14].

---

## 5 Conclusion

As reviewed above, there are a wide variety of time-resolved flow cytometers as well as fluorescence lifetime applications that can be used for cell counting and sorting. Although these techniques are not marketed commercially, they are now enhancing the way flow cytometry can be utilized. It is beneficial as well that detecting fluorescence lifetimes or decay-kinetic dependent values with a flow cytometer does not remove the ability to detect traditional data parameters such as peak intensity, pulse width, and pulse area. Therefore, modulated or pulsed excitation light sources merely add to the parameter space for cytometric data collection and might even be adopted on new spectral cytometry or imaging cytometry systems.

The addition of fluorescence lifetime detection via digital or other data processing methods increases the total amount of information available to researchers. Off-line time-resolved parameters that may be of value to single cell analyses are possible with specialty computer programs that incorporate algorithms which process the

time-resolved signals into meaningful averages (e.g., regression of exponential decay into a lifetime value or Fourier analysis of multi-frequency signals into phase and modulation values). Post-processing requires MATLAB or another software program that can import digitized data and reprocess the numbers into list mode values whereby the fluorescence lifetime is the graphed parameter. In contrast, real-time fluorescence lifetime parameters are processed on-chip with programmable digital data acquisition systems (i.e., combined with FPGAs) using programming languages with simple and rapid algorithms (e.g., discrete Fourier transforms, Goertzel algorithms). The on-line analyses are particularly useful for cell sorting at nominal sort rates.

Future work in fluorescence lifetime measurements with a flow cytometer might involve more complicated approaches such as non-modulated waveform analyses, higher frequency modulation, digital heterodyning, or frequency aliasing, for example. Frequencies higher than the Nyquist frequency can be analyzed by exploiting aliased signals because this approach circumvents the limitations of analyzing frequencies beyond the digitization rate of the data system. It is desirable to inspect higher modulation frequencies because they lead to larger phase perturbations for the short fluorescence lifetime values (i.e., 100–500 ps). With aliasing, frequencies above any inherent Nyquist limit can be available as fold over frequencies, therefore frequencies higher than the Nyquist limit can be accessed. Aliasing is but only one example of how frequency-domain systems can be improved or expanded upon for better resolution of the fluorescence lifetime as a parameter.

In terms of the application space, future work may likely involve ways in which the fluorescence lifetime can be used to discriminate among spectrally overlapping signals, which is a recurring challenge in flow cytometry. Most applications lead back to the fact that the fluorescence lifetime is independent of fluorophore concentration and spectral emission and excitation wavelengths. Also emerging are single cell applications that build on measurements made using FLIM. Many opportunities remain for flow cytometry, which offers high-throughput cell counting or sorting measurements not present with lifetime microscopy. One untapped application is the measurement of autofluorescence lifetime shifts during bound and un-bound states of the metabolite, nicotinamide adenine dinucleotide (NADH). This specie is not only brightly autofluorescent but also has a unique free and protein-bound fluorescence lifetime [71]. Cytometry measurements of NADH can lead to high-throughput metabolic mapping of single cells and therefore add to current knowledge about cellular transformation from glycolytic states to oxidative phosphorylation. With the changing NADH decay kinetics, there is a need to detect when and how much of an intracellular species experiences a shift in its fluorescence lifetime. The quantification of multiple fluorescence lifetimes is

therefore quite valuable and can be applied to other intrinsic or extrinsic fluorophores.

Overall the rise in the number of flow cytometry assays that incorporate time-resolved measurements suggests a growing interest in high-throughput tools that count or sort cells based on the fluorescence lifetime. This chapter summarizes the various ways in which cytometrists have implemented lifetime measurements as well as the modern application space for these systems. A variety of machinations can be taken to transform existing cytometers into time-resolved systems or to build “ground-up” cytometers with this capability. Regardless, new analysis approaches and applications such as phasor plots combined with FRET should evolve in parallel to best leverage this measurement into an approach that provides meaningful biological information.

## References

1. Steinkamp JA, Yoshida TM, Martin JC (1993) Flow cytometer for resolving signals from heterogeneous fluorescence emissions and quantifying lifetime in fluorochrome-labeled cells/particles by phase-sensitive detection. *Rev Sci Instrum* 64(12):3440–3450
2. Lakowicz JR, Szmazinski H (1993) Fluorescence lifetime-based sensing of pH, Ca<sup>2+</sup>, K<sup>+</sup> and glucose. *Sens Actuators B Chem* 11(1):133–143
3. Pinsky BG, Ladasky JJ, Lakowicz JR, Berndt K, Hoffman RA (1993) Phase-resolved fluorescence lifetime measurements for flow cytometry. *Cytometry A* 14(2):123–135
4. Steinkamp JA, Crissman HA (1993) Resolution of fluorescence signals from cells labeled with fluorochromes having different lifetimes by phase-sensitive flow cytometry. *Cytometry A* 14(2):210–216
5. Lakowicz JR (2013) Principles of fluorescence spectroscopy. Springer Science & Business Media, New York
6. Deka C, Sklar LA, Steinkamp JA (1994) Fluorescence lifetime measurements in a flow cytometer by amplitude demodulation using digital data acquisition technique. *Cytometry A* 17(1):94–101
7. Steinkamp JA, Keij JF (1999) Fluorescence intensity and lifetime measurement of free and particle-bound fluorophore in a sample stream by phase-sensitive flow cytometry. *Rev Sci Instrum* 70(12):4682–4688
8. Steinkamp JA, Lehnert BE, Lehnert NM (1999) Discrimination of damaged/dead cells by propidium iodide uptake in immunofluorescently labeled populations analyzed by phase-sensitive flow cytometry. *J Immunol Methods* 226(1):59–70
9. Houston JP, Naivar MA, Freyer JP (2010) Digital analysis and sorting of fluorescence lifetime by flow cytometry. *Cytometry A* 77(9):861–872
10. Sands B, Jenkins P, Peria WJ, Naivar M, Houston JP, Brent R (2014) Measuring and sorting cell populations expressing isospectral fluorescent proteins with different fluorescence lifetimes. *PLoS One* 9(10):e109940
11. Cao R, Pankayatselvan V, Houston JP (2013) Cytometric sorting based on the fluorescence lifetime of spectrally overlapping signals. *Opt Express* 21(12):14816–14831
12. Gohar AV, Cao R, Jenkins P, Li W, Houston JP, Houston KD (2013) Subcellular localization-dependent changes in EGFP fluorescence lifetime measured by time-resolved flow cytometry. *Biomed Opt Express* 4(8):1390–1400
13. Jenkins P, Naivar MA, Houston JP (2015) Toward the measurement of multiple fluorescence lifetimes in flow cytometry: maximizing multi-harmonic content from cells and microspheres. *J Biophotonics* 8(11–12):908–917. doi:10.1002/jbio.201400115
14. Nedbal J, Visitkul V, Ortiz-Zapater E, Weitsman G, Chana P, Matthews DR, Ng T, Ameer-Beg SM (2015) Time-domain microfluidic fluorescence lifetime flow cytometry for high-throughput Förster resonance energy transfer screening. *Cytometry A* 87(2):104–118
15. Okabe K, Inada N, Gota C, Harada Y, Funatsu T, Uchiyama S (2012) Intracellular temperature mapping with a fluorescent polymeric thermometer and fluorescence lifetime imaging microscopy. *Nat Commun* 3:705

16. Deka C, Lehnert BE, Lehnert NM, Jones GM, Sklar LA, Steinkamp JA (1996) Analysis of fluorescence lifetime and quenching of FITC-conjugated antibodies on cells by phase-sensitive flow cytometry. *Cytometry A* 25 (3):271–279
17. Gopich IV, Szabo A (2012) Theory of the energy transfer efficiency and fluorescence lifetime distribution in single-molecule FRET. *Proc Natl Acad Sci U S A* 109(20):7747–7752
18. Sailer BL, Valdez JG, Steinkamp JA, Darzynkiewicz Z, Crissman HA (1997) Monitoring uptake of ellipticine and its fluorescence lifetime in relation to the cell cycle phase by flow cytometry. *Exp Cell Res* 236(1):259–267
19. Steinkamp JA, Valdez YE, Lehnert BE (2000) Flow cytometric, phase-resolved fluorescence measurement of propidium iodide uptake in macrophages containing phagocytized fluorescent microspheres. *Cytometry* 39(1):45–55
20. Sailer BL, Nastasi AJ, Valdez JG, Steinkamp JA, Crissman HA (1997) Differential effects of deuterium oxide on the fluorescence lifetimes and intensities of dyes with different modes of binding to DNA. *J Histochem Cytochem* 45 (2):165–175
21. Sailer BL, Nastasi AJ, Valdez JG, Steinkamp JA, Crissman HA (1996) Interactions of intercalating fluorochromes with DNA analyzed by conventional and fluorescence lifetime flow cytometry utilizing deuterium oxide. *Cytometry A* 25(2):164–172
22. Sailer BL, Steinkamp JA, Crissman HA (1997) Flow cytometric fluorescence lifetime analysis of DNA-binding probes. *Eur J Histochem* 42:19–27
23. Sailer BL, Valdez JG, Steinkamp JA, Crissman HA (1998) Apoptosis induced with different cycle-perturbing agents produces differential changes in the fluorescence lifetime of DNA-bound ethidium bromide. *Cytometry A* 31 (3):208–216
24. Keij JF, Bell-Prince C, Steinkamp JA (1999) Simultaneous analysis of relative DNA and glutathione content in viable cells by phase-resolved flow cytometry. *Cytometry A* 35 (1):48–54
25. Steinkamp JA (2001) Time-resolved fluorescence measurements. *Curr Protoc Cytom*:1.15.11–11.15.16
26. Cui HH, Valdez JG, Steinkamp JA, Crissman HA (2003) Fluorescence lifetime-based discrimination and quantification of cellular DNA and RNA with phase-sensitive flow cytometry. *Cytometry A* 52(1):46–55. doi:10.1002/cyto.a.10022
27. Digman MA, Caiolfa VR, Zamai M, Gratton E (2008) The phasor approach to fluorescence lifetime imaging analysis. *Biophys J* 94(2):L14–L16. doi:10.1529/biophysj.107.120154
28. Skala MC, Riching KM, Gendron-Fitzpatrick A, Eickhoff J, Eliceiri KW, White JG, Ramanujam N (2007) In vivo multiphoton microscopy of NADH and FAD redox states, fluorescence lifetimes, and cellular morphology in precancerous epithelia. *Proc Natl Acad Sci U S A* 104 (49):19494–19499. doi:10.1073/pnas.0708425104
29. Periasamy A, Elangovan M, Elliott E, Brautigan DL (2002) Fluorescence lifetime imaging (FLIM) of green fluorescent fusion proteins in living cells. *Methods Mol Biol* 183:89–100. doi:10.1385/1-59259-280-5-089
30. Chen Y, Mills JD, Periasamy A (2003) Protein localization in living cells and tissues using FRET and FLIM. *Differentiation* 71 (9–10):528–541. doi:10.1111/j.1432-0436.2003.07109007.x
31. Sun Y, Periasamy A (2015) Localizing protein-protein interactions in living cells using fluorescence lifetime imaging microscopy. *Methods Mol Biol* 1251:83–107. doi:10.1007/978-1-4939-2080-8\_6
32. Lubbeck JL, Dean KM, Ma H, Palmer AE, Jimenez R (2012) Microfluidic flow cytometer for quantifying photobleaching of fluorescent proteins in cells. *Anal Chem* 84(9):3929–3937
33. Manna P, Jimenez R (2015) Time and frequency-domain measurement of ground-state recovery times in red fluorescent proteins. *J Phys Chem B* 119(15):4944–4954
34. Boens N, Qin W, Basarić N, Hofkens J, Ameloot M, Pouget J, Lefèvre J-P, Valeur B, Gratton E, van de Ven M, Silva ND, Engelborghs Y, Willaert K, Sillen A, Rumbles G, Phillips D, AJWG V, van Hoek A, Lakowicz JR, Malak H, Gryczynski I, Szabo AG, Krajcarski DT, Tamai N, Miura A (2007) Fluorescence lifetime standards for time and frequency domain fluorescence spectroscopy. *Anal Chem* 79 (5):2137–2149. doi:10.1021/ac062160k
35. Becker W (2012) Fluorescence lifetime imaging—techniques and applications. *J Microsc* 247 (2):119–136
36. Houston JP, Naivar MA, Jenkins P, Freyer JP (2012) Capture of fluorescence decay times by flow cytometry. *Curr Protoc Cytom*:1.25.1–1.25.21
37. Steinkamp JA, Crissman HA (1993) Resolution of fluorescence signals from cells labeled with fluorochromes having different lifetimes by phase-sensitive flow cytometry. *Cytometry* 14(2):210–216
38. Pinsky BG, Ladasky JJ, Lakowicz JR, Berndt K, Hoffman RA (1993) Phase-resolved

- fluorescence lifetime measurements for flow cytometry. *Cytometry* 14(2):123–135
39. Steinkamp JA (1994) Phase-sensitive detection methods for resolving fluorescence emission signals and directly quantifying lifetime. *Methods Cell Biol* 42:627
  40. Deka C, Cram LS, Habbersett R, Martin JC, Sklar LA, Steinkamp JA (1995) Simultaneous dual-frequency phase-sensitive flow cytometric measurements for rapid identification of heterogeneous fluorescence decays in fluorochrome-labeled cells and particles. *Cytometry A* 21(4):318–328
  41. Keij JF, Steinkamp JA (1998) Flow cytometric characterization and classification of multiple dual-color fluorescent microspheres using fluorescence lifetime. *Cytometry A* 33(3):318–323
  42. Sailer BL, Nastasi AJ, Valdez JG, Steinkamp JA, Crissman HA (1998) Interactions of intercalating fluorochromes with DNA analyzed by conventional and fluorescence lifetime flow cytometry utilizing deuterium oxide. *Cytometry A* 25(2):164–172
  43. Jenkins PL, Freyer JP, Naivar MS, Arteaga A, Houston JP (2011) Flow cytometric separation of spectrally overlapping fluorophores using multifrequency fluorescence lifetime analysis. In: SPIE BiOS., 2011. International Society for Optics and Photonics, pp 790216–790218
  44. Stringari C, Cinquin A, Cinquin O, Digman MA, Donovan PJ, Gratton E (2011) Phasor approach to fluorescence lifetime microscopy distinguishes different metabolic states of germ cells in a live tissue. *Proc Natl Acad Sci U S A* 108(33):13582–13587. doi:10.1073/pnas.1108161108
  45. Colyer RA, Lee C, Gratton E (2008) A novel fluorescence lifetime imaging system that optimizes photon efficiency. *Microsc Res Tech* 71(3):201–213. doi:10.1002/jemt.20540
  46. Dean KM, Davis LM, Lubbeck JL, Manna P, Palmer AE, Jimenez R (2014) Microfluidic flow cytometer for multiparametric screening of fluorophore photophysics. *Opt Soc Am*:1–3
  47. Li W, Vacca G, Castillo M, Houston KD, Houston JP (2014) Fluorescence lifetime excitation cytometry by kinetic dithering. *Electrophoresis* 35(12–13):1846–1854
  48. Lu Y, Lu J, Zhao J, Casido J, Raymo FM, Yuan J, Yang S, Leif RC, Huo Y, Piper JA (2014) On-the-fly decoding luminescence lifetimes in the microsecond region for lanthanide-encoded suspension arrays. *Nat Commun* 5:3741
  49. Lu Y, Zhao J, Zhang R, Liu Y, Liu D, Goldys EM, Yang X, Xi P, Sunna A, Lu J (2014) Tunable lifetime multiplexing using luminescent nanocrystals. *Nat Photonics* 8(1):32–36
  50. Ding M, Chen D, Ma D, Liu P, Song K, Lu H, Ji Z (2015) Tuning the upconversion luminescence lifetimes of KYb2F7: Ho<sup>3+</sup> nanocrystals for optical multiplexing. *Chem Phys Chem* 16(18):3784–3789
  51. Cao R, Naivar MA, Wilder M, Houston JP (2014) Expanding the potential of standard flow cytometry by extracting fluorescence lifetimes from cytometric pulse shifts. *Cytometry A* 85(12):999–1010
  52. Deka C, Steinkamp JA (1996) Time-resolved fluorescence-decay measurement and analysis on single cells by flow cytometry. *Appl Opt* 35(22):4481–4489
  53. Steinkamp JA, Keij JF (1998) Fluorescence lifetime measurement of free and cell/particle-bound fluorophore by phase-sensitive flow cytometry. In: BiOS'98 international biomedical optics symposium. International Society for Optics and Photonics, pp 154–161
  54. Steinkamp JA, Lehnert NM, Keij JF, Lehnert BE (1999) Enhanced immunofluorescence measurement resolution of surface antigens on highly autofluorescent, glutaraldehyde-fixed cells analyzed by phase-sensitive flow cytometry. *Cytometry A* 37(4):275–283
  55. Tirri ME, Wahlroos R, Meltola NJ, Toivonen J, Hänninen PE (2006) Effect of polystyrene microsphere surface to fluorescence lifetime under two-photon excitation. *J Fluoresc* 16(6):809–816
  56. Jin D, Connally R, Piper J (2007) Practical time-gated luminescence flow cytometry. I: Concepts. *Cytometry A* 71(10):783–796
  57. Jones T, Jenkins P, Houston J (2010) Resolving multiple fluorescence decays from single cytometric events. In: Biomedical optics. Optical Society of America, p BTuD113p
  58. Lu Y, Xi P, Piper JA, Huo Y, Jin D (2012) Time-gated orthogonal scanning automated microscopy (OSAM) for high-speed cell detection and analysis. *Sci Rep* 2:837
  59. Buschke DG, Resto P, Schumacher N, Cox B, Tallavajhula A, Vivekanandan A, Eliceiri KW, Williams JC, Ogle BM (2012) Microfluidic sorting of microtissues. *Biomicrofluidics* 6(1):014116
  60. Dahal E, Cao R, Jenkins P, Houston JP (2014) High-throughput measurement of the long excited-state lifetime of quantum dots in flow cytometry. In: SPIE BiOS. International Society for Optics and Photonics, pp 89470S–89478
  61. Léonard J, Dumas N, Caussé J, Maillot S, Giannakopoulou N, Barre S, Uhring W

- (2014) High-throughput time-correlated single photon counting. *Lab Chip* 14 (22):4338–4343
62. Bene L, Szöllösi J (2014) À la Fizeau in flow: Pulse shape-assisted fluorescence lifetime. *Cytometry A* 85(12):991–994
63. Dean KM, Davis LM, Lubbeck JL, Manna P, Friis P, Palmer AE, Jimenez R (2015) High-speed multiparameter photophysical analyses of fluorophore libraries. *Anal Chem* 87 (10):5026–5030
64. Suzuki M, Sakata I, Sakai T, Tomioka H, Nishigaki K, Tramier M (2015) A high-throughput direct FRET-based assay for analyzing apoptotic proteases using flow cytometry and fluorescence-lifetime measurements. *Anal Biochem* 491:10
65. Sailer BL, Steinkamp JL, Crissman HA (1998) Flow cytometric lifetime analysis of DNA-binding probes. *Eur J Histochem* 48:19–27
66. Yang Z, Shcherbakova D, Verkhusha V, Houston J (2016) Developing a time-resolved flow cytometer for fluorescence lifetime measurements of near-infrared fluorescent proteins. In: Conference on lasers and electro-optics CLEO 2016, San Jose, CA. Optical Society of America
67. Hinde E, Digman MA, Welch C, Hahn KM, Gratton E (2012) Biosensor Förster resonance energy transfer detection by the phasor approach to fluorescence lifetime imaging microscopy. *Microsc Res Tech* 75 (3):271–281. doi:10.1002/jemt.21054
68. Chigaev A, Buranda T, Dwyer DC, Prossnitz ER, Sklar LA (2003) FRET detection of cellular  $\alpha 4$ -integrin conformational activation. *Biophys J* 85(6):3951–3962. doi:10.1016/S0006-3495(03)74809-7
69. Chigaev A, Smagley Y, Haynes MK, Ursu O, Bologa CG, Halip L, Oprea T, Waller A, Carter MB, Zhang Y (2015) FRET detection of lymphocyte function-associated antigen-1 conformational extension. *Mol Biol Cell* 26(1):43–54
70. Chigaev A, Blenc AM, Braaten JV, Kumaraswamy N, Kepley CL, Andrews RP, Oliver JM, Edwards BS, Prossnitz ER, Larson RS (2001) Real time analysis of the affinity regulation of  $\alpha 4$ -integrin the physiologically activated receptor is intermediate in affinity between resting and  $Mn^{2+}$  or antibody activation. *J Biol Chem* 276(52):48670–48678
71. Lakowicz JR, Szmacinski H, Nowaczyk K, Johnson ML (1992) Fluorescence lifetime imaging of free and protein-bound NADH. *Proc Natl Acad Sci U S A* 89(4):1271–1275